CALIFORNIA POLYTECHNIC STATE UNIVERSITY (CALPOLY)

Technical Turbine Design Report

2021 DOE Collegiate Wind Competition

May 23, 2021

Aero Team
Jessica Dent (Lead)
Josephine Maiorano

Electrical Team
Grayson Capers (Lead)
Shane Alayvilla
Jonathan Yu
Matthew Renati

Sophie Spencer – **Team Lead**

Mechanical Team
Zachary Dunkleberger (Lead)
Elizabeth Costley
Jeff Larson
Kinsale Sproule
Milo Klein
Nora Riedinger

Advisors
Dr. Andrew Kean – Principal Investigator
Prof. Ali Dehghan Banadaki – Faculty Advisor
Dr. Patrick Lemieux – Faculty Advisor
Paulo Iscold & Nandeesh Hiremath – Wind Tunnel Managers

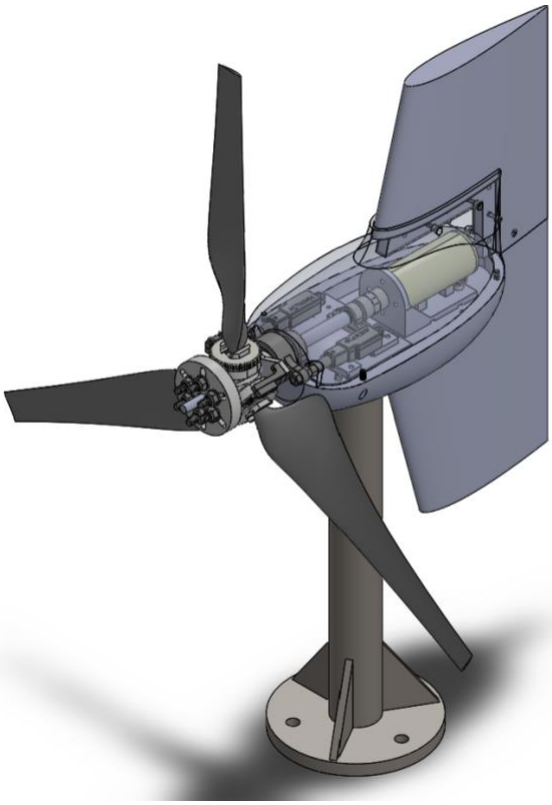

WIND POWER
CAL POLY, SAN LUIS OBISPO, CA

TABLE OF CONTENTS

1.0 EXECUTIVE SUMMARY

In this report, the California Polytechnic State University, San Luis Obispo Wind Power team (CPWP) outlines the technical design decisions, analysis, and testing results of the turbine development component of the Department of Energy's 2021 Collegiate Wind Competition (CWC). The CWC has tasked CPWP with designing, manufacturing, and testing a small-scale wind turbine to meet the dimensional and loading engineering specifications outlined in the CWC Rules and Requirements [1]. The turbine should ideally meet a set of performance tasks: cut-in wind speed, power curve performance, control of rated power, safety, and durability tasks. Given the disruptions from 2020-2021 public health restrictions, the turbine should also be designed for distributed manufacturability.

Section *2.0 Technical Design* presents detailed information on the aerodynamic, mechanical, and electrical design decisions and analyses made by CPWP. This section outlines the overall design objectives as well as those specific to each subsection. First, the rotor aerodynamics design process is outlined presenting the methods used to achieve the final airfoil, chord, and twist distribution. Additionally, both the structural and aerodynamic analysis is provided to ensure the turbine meets the CWC safety requirements and optimizes rotor performance. Subsequently, the design of the mechanical systems including, the pitching system, drivetrain, support structures, and yawing system, is showcased with both structural and functional analysis. Next, the electrical system section documents the design, build, and test of each of the components that make up the electrical subsystem. In addition, the controls analysis and software documentation are outlined including how each subsystem will satisfy each of the turbine testing tasks.

Section *3.0 Testing* outlines the field and wind tunnel testing CPWP has been able to accomplish and their respective results. With limited lab and wind tunnel accessibility this year, field testing has been largely utilized to ensure the functional and structural performance of the turbine as well as for design iteration for optimizing aerodynamic performance. Wind tunnel testing results are outlined as well as how the results influenced the team's next steps in improving performance.

Section *4.0 Conclusion* summarizes CPWP's accomplishments and turbine performance results. Additionally, this section illustrates what the team learned from their first year competing in the CWC and outlines future steps that will be taken to optimize turbine performance.

2.0 TECHNICAL DESIGN

The Cal Poly Wind Power (CPWP) team was challenged by the CWC to design, build, and test a wind turbine that could produce power under the various testing conditions outlined in the CWC Rules and Requirements [1]. A wind turbine is designed to extract as much energy out of the wind as possible by utilizing blade aerodynamics to rotate a shaft, which in turn drives a generator to produce electricity. The technical design of the turbine outlined in the following sections are broken down by the main components of the turbine: the blades, pitching mechanism, drivetrain, support structures and yaw mechanism, and finally the electrical and controls systems.

2.1 Overall Design Objective

Like most teams, the CPWP team needed to overcome unique limitations due to limited access to the campus machine shops and testing facilities as well as limited ability to meet up in person to work on the design. Being a brand-new team to the competition, the Cal Poly team also needed to complete all design work from scratch. A majority of this competition year was dedicated to the technical design of the turbine. The team did extensive research through the turbine design reports of previous competition teams. Common challenges previous teams experienced were noted when determining the design objectives for the CPWP 2021 turbine. Challenges identified include difficulty achieving low cut-in wind speeds and stalling in high wind speeds.

The winning report from the 2020 competition influenced the team's design decisions by encouraging the ambitious design of a variable pitch turbine to optimize the power output of the turbine, especially at low speeds. The pitching mechanism would also allow the turbine to increase the angle of attack at lower wind speeds and aid in reducing the cut in wind speed. Additionally, it could be used to pitch the blades to limit the rotor speed in the control of rated rotor speed task and "park" the turbine in extreme wind conditions. The team emphasized selecting a generator which exhibited low startup torque and thus provided a low cut in wind speed. The 2021 Cal Poly turbine was designed to be a 40-Watt variable-pitch horizonal axis wind turbine. The theoretical maximum power available in the wind is higher than this, however the team assumed that this first turbine attempt would have significant losses on top of the Betz limit due to lack of experience, so the goal power production was set at 40W.

2.2 Blade Design Objective

The blade design is integral to producing the desired turbine performance, so the team placed emphasis on iteration of this aspect of the turbine to optimize the aerodynamic performance of the blades. Throughout the blade design process, the team emphasized repeated testing to produce blades with a low cut-in wind speed and reliable performance in variable wind conditions. The team chose 11 m/s as the rated wind speed for the turbine, which affected the chosen tip speed ratio (TSR) and blade geometry.

The team originally chose a TSR of 5 since the generator was not yet fully specified, however later learned through experimentation that lower tip speed ratios perform better with real-world conditions for turbines this small and fast moving. The final TSR selected was 3.75, to align the peak power producing performance of the blades with the design generator speed of about 2100 rpm.

2.2.1 Blade Design

The first consideration was which airfoil to use. After extensive research through research papers and available small wind turbine data, the team used the software Q-Blade to compare the lift, drag, lift over drag coefficients (C_L/C_D) versus alpha, and power coefficients of each airfoil. The airfoil which exhibited the highest C_L/C_D versus alpha at low angles of attack was selected. The blades were designed using blade element momentum theory [2, 3]. This method was built into a MATLAB script which was developed entirely by the student team. The MATLAB code uses a numerical method [3] to iterate the angle of attack

for each blade element by solving for the intersection of that individual element's lift coefficient (black) with the empirically derived C_L versus alpha curve for that airfoil (blue), as shown in Figure 1.

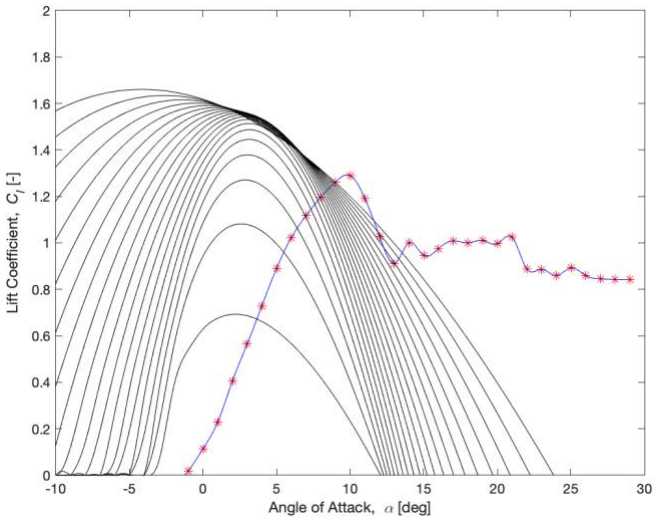

Figure 1. C_L and Angle of Attack Iteration at Each Blade Element to Solve for Blade Twist Distribution.

Additionally, the code outputs the necessary chord lengths and twist angles for the inputs of the desired tip speed ratio (TSR), and the predicted lift, drag, and moment coefficients produced via QBlade for the specified airfoil. The code was designed to analyze the blade with 2 or more different airfoils, such as a thicker root airfoil for greater structural integrity. The Reynolds number that the team used was about 50,000, which was determined using an average chord length which could be reasonably manufactured and withstand the loads induced at 22 m/s wind speeds.

The Cp-Lambda plot using the chosen airfoil for blade design, SD7043, defines the performance of the turbine's theoretical performance over a range of tip speed ratios. The Cp-Lambda plot of the final rotor design is shown in Figure 2. For most blade designs, the power coefficient peaked at a TSR of about 7, however with the incredibly small rotor diameter restrictions, the team determined that a lower rpm was necessary for both safety and practicality. The team chose a design TSR of 3.75 instead.

The blade manufacturing process was considered by a senior project team, and it was concluded that due to the limited machine shop access, experience with composites, and CNC milling, the most reliable route for blade manufacture would be to 3D print them. The team determined that the best materials for 3D printing were ABS or an SLA resin. The ABS was determined to be more lightweight and less brittle, however less structurally sound, and with significantly rougher surface finish. The application of a coating to smooth the surface finish was considered, however, the risk of significant mass imbalance was of concern. The team decided to use the SLA resin printed blades for final prototypes.

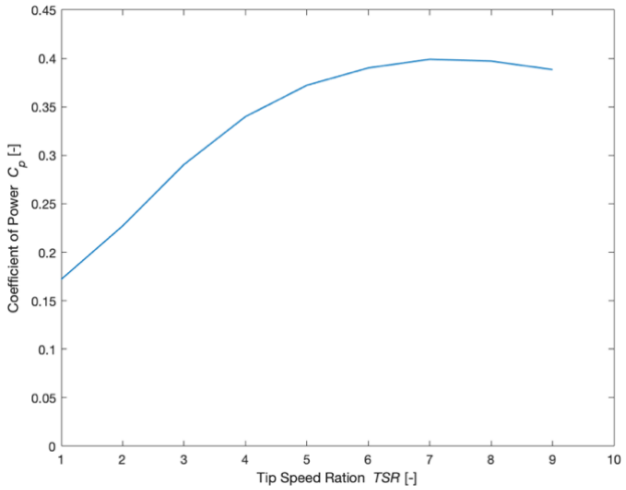

Figure 2. Power Coefficient versus Tip Speed Ratio of Turbine Using SD7043 Airfoils.

2.2.2 Blade Structural Analysis

The team assessed that the most critical loading would be at the cut-out wind speed during the safety test, at 22 m/s. Since this is the team's first time competing in the Collegiate Wind Competition, conservative values were used and a broad safety factor of 2.0 was applied to estimated maximum loads. This made the safety factor even higher on the turbine when in a static conditions, such as parked in high winds, and during conditions at or below the rated speed. The loads were calculated using the thrust, torque, drag, and lift coefficients from the BEM analysis at 22 m/s and are listed in Table 1.

Table 1. Loading on Blades Operating at Maximum Wind Speed.

Load	Magnitude	Units
F_A – Axial Force	33.5	N
F_N – Flapwise (Lift) Force	16.0	N
F_T - Edgewise (Drag) Force	3.1	N
M_P - Pitching Moment	-0.8	N-m
M_X - Edgewise Moment	0.4	N-m
M_Y - Flapwise Moment	0.2	N-m

The combined loading on each blade while operating can be broken down into three forces and three moments, characterized by being axial, flapwise, or edgewise. The diagram in Figure 3 shows the direction of these loads with reference to the naming convention in Table 1.

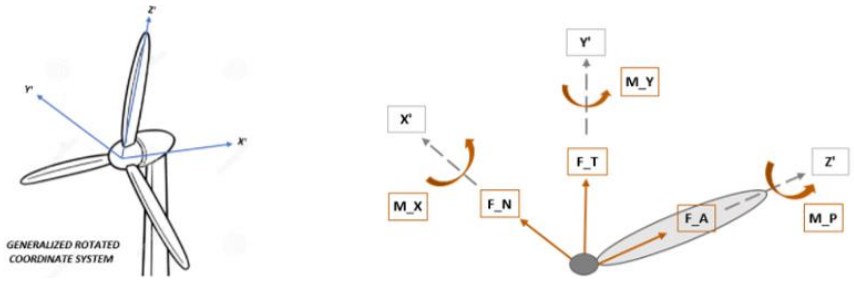

Figure 3. Diagram of External Forces and Moments Applied to Each Blade.

To analyze the effects of this loading, the team conducted finite element analysis (FEA) on the blade geometries, with both operational and parked loading conditions, to ensure that they would not experience stresses greater than the yield strength of the material. The loads used in FEA also utilize the same safety factors as previously mentioned. Torsion induced in the shaft from the blades being parked was taken under consideration in the shaft design, see 2.4.1 Shaft Design for more details. During the stationary analysis, the drag force on the blades in the edgewise direction from rotational motion were negligible.

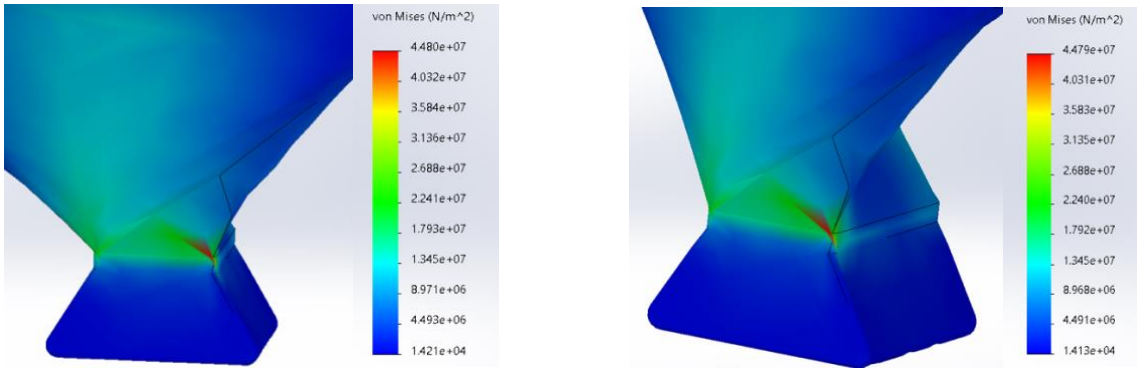

(a) Operational Loading (b) Stationary Loading

Figure 4. Results of the Operational and Parked Loading FEA Studies at 22 m/s Wind Speed.

The blades were assessed using a 60% reduced material strength for the ABS resin, the material properties for which were estimated from the manufacturer's datasheets. The reduction in strength is to account for the loss of strength due to the material being 3D printed. The highest stress concentrations were around the root as expected, as seen in Figure 4. The highest expected stresses were well below the yield strength of the material. The blades passed both simulations and real-world testing, leading the team to confirm that the rotor design was structurally sound.

2.2.3 Aerodynamic Analysis

Most of the aerodynamic analysis was done first by simulation and then validated in real-world testing. The majority of the real testing was done on a fixed-pitch turbine, leading to insights about the aerodynamic behavior of the turbine. With the focus on reducing the cut-in speed, the team found that increasing the angle of attack for low wind speeds would increase the torque produced by the rotor and thus lead to a lower cut-in wind speed with slightly higher power. This was validated during simple comparative testing of a set of blades early in the design process, using static hubs with either 0 or 15 degrees angle of attacks.

Since the turbine was designed as a variable pitch, further aerodynamic analysis of the blade performance at a range of pitch angles was necessary. This was again performed using the team's custom MATLAB script. To evaluate the best pitching angle for each wind speed, plots of the torque and power coefficient versus a range of pitch angles was used and are shown in Figure 5. The team found that the effects of the pitch angle on torque becomes more pronounced as the wind speeds increase, while the optimum pitch angle for a high power coefficient decreases with increased wind speeds. This led the team to determine that the turbine should start at higher pitch angles at low wind speeds, and then decrease the pitch to zero degrees when the turbine hits the rated wind speed of 11 m/s.

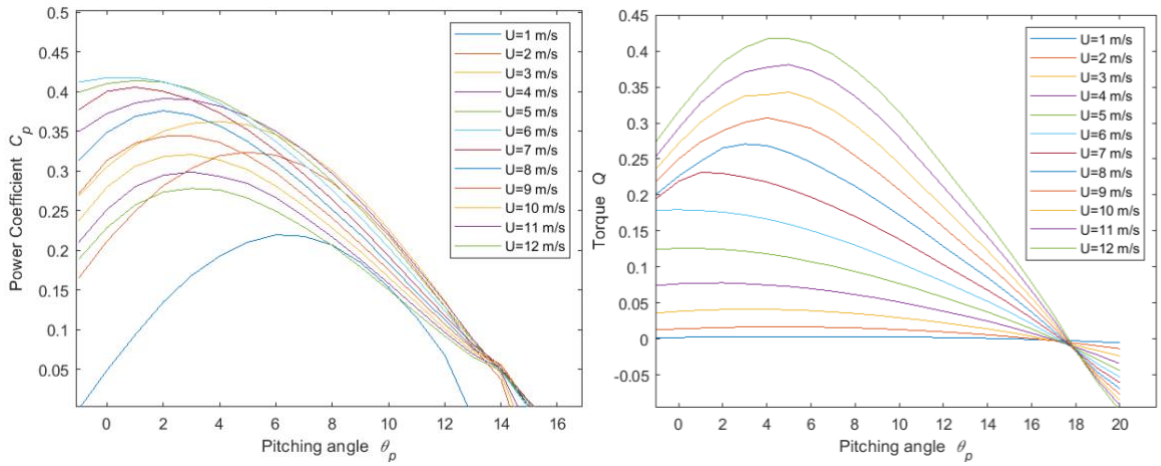

(a) Power Coefficient vs. Pitch Angle (b) Torque vs. Pitch Angle

Figure 5. Plots of Cp vs. Pitch Angle and Torque vs. Pitch Angle.

Various blade geometries were compared by 3D-printing a fixed-pitch rotor set and documenting the performance at low and high wind speeds. Comparative tests were completed with a high-powered fan. The team printed six different rotor sets to test, including ones with a factor applied to uniformly increase the blade's chord length. The team had noticed in prior testing that blades with larger chords operated at higher rpms. The results of the testing showed that blades with a large chord factor produced the most power.

As a result of final testing, the blades chosen for the team's final turbine used blades with only SD7043 airfoils and a chord factor of 4.25 applied to uniformly increase the length of the chords. With more time available, the team would have liked to further iterate root airfoils within the same family to further improve performance by generating more lift at the root of the blade.

2.3 Pitching Mechanism

A blade pitching system on a turbine can improve its efficiency and reduce the likelihood of failure when operating in extreme wind speeds. Primarily, the pitching system helps maintain a constant mechanical power from the rotor to maximize the power generation of the turbine's generator. The designed pitching mechanism achieves this by adjusting each blade's angle of attack with respect to the wind simultaneously. The angle of attack directs the lift and drag forces induced by the wind, which then controls the rotor speed. This enables the generator to produce consistent electrical power at or above its rated rotational speed.

2.3.1 Pitching Mechanism Design

To maintain reliable power, the pitching mechanism must pitch accurately and rapidly and maintain a low power draw to improve the efficiency of the turbine. Key structural considerations include reducing inertia about the rotational axis as well as reducing the moment on the cantilevered end of the turbine shaft. The final pitching system subassembly is shown in Figure 6.

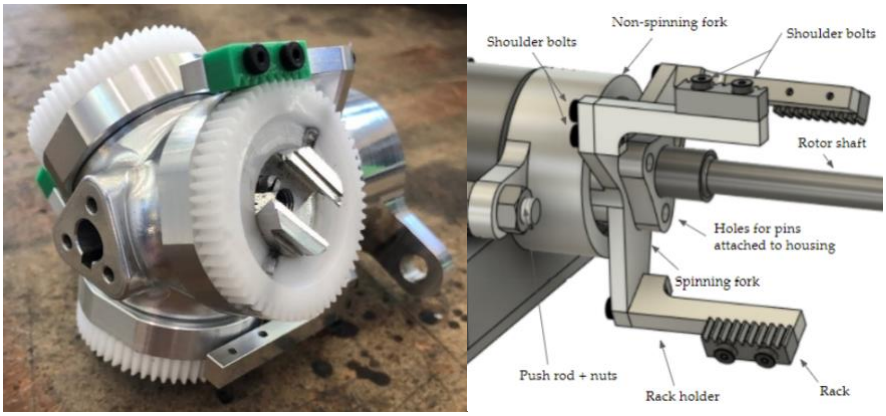

Figure 6. Assembled Pitching Mechanism Subassembly

The pitching mechanism design was evaluated using the technical specifications given in Table 2. Ultimately, the rack-and-pinion design was chosen to focus on mechanical simplicity and reliability, rather than making the assembly more compact. The final design of the pitching mechanism is a system that is actuated by two linear actuators mounted inside the nacelle, which are connected by pushrods to the relative motion subassembly outside the nacelle.

Table 2. Pitching Mechanism Technical Requirements.

Requirement	Value	Unit
Pitch Rate	2	deg/s
Pitch Torque	0.8	N-m
Pitch Range	20	deg
Active Power Draw	5	W
Standby Power Draw	1	W
Subsystem Mechanical Efficiency	90	%
Pitch Resolution	0.5	deg

The relative motion subassembly allows the collars connected to the actuators to slide along the rotor shaft axis. While the rack and pinions spin, the relative motion sub assembly allows for linear movement of the racks and causes pitching of the blades. The blade mounting subassembly then constrains the blades in all degrees of freedom, except for rotation about the pitch axis, and establishes the primary load path from the blades to the rotor shaft.

While the team focused on mechanical reliability, CPWP also worked to limit the hub's diameter to achieve better aerodynamic performance by decreasing the radial distance from the axis of the rotor shaft to the start of the blade. This also lowers the rotational inertia of the outboard turbine system. The relative motion subassembly rack mounting was designed for easy manufacturability and emphasized using stock material that is low cost. In addition, three pins were used in the hub housing to constrain rotational degrees of freedom of the spinning fork. Using pins helped shorten the tolerance stack for the assembly so that the angular position of the racks relative to the pinions could be better controlled.

To select the linear actuators, calculations were performed for the linear travel, linear velocity, and tangential force required from the actuator for various pinion radii. Ultimately, the 6 V DC Actuonix L12-R Micro Linear Servos for RC and Arduino with 210:1 gear reduction were chosen as the actuators for the final design. The L12-R also features closed-loop position feedback that easily interfaces with an Arduino control system.

2.3.2 Pitching Mechanism Analysis

The pitching mechanism underwent static testing to ensure the blade connection subassembly and entire rotating subassembly would withstand the loads they would experience during operation. This was done by applying loads using fish scales in the directions of the anticipated maximum loads. The static testing setup can be seen in Figure 7. The static testing resulted in the failure of the 3D printed dovetail base, used to attach the blades to the hub. The team addressed this issue by machining the final dovetail bases out of aluminum.

Figure 7. Pitching Mechanism Static Loading Apparatus

2.4 Drive Train Components

The drive train consists of the shaft, bearings, rotor balancing mechanism, couplings, and appropriate mounting and housing hardware for the listed components. The drive train needs to efficiently transmit power from the hub to the generator while withstanding the cyclic loads created during operation, avoiding vibration, and providing sufficient alignment so as not to impart undue stresses or wear on the components.

2.4.1 Shaft Design

When designing the shaft, the team began by analyzing the expected loads the shaft would be subjected to. These can be separated into parked loads which are always present, and operational loads. The torque from the wind, T_w, the gyroscopic moment caused by the interaction between the rotation of the shaft and the rotation of the yaw and the reactionary torque, T_r, are the only additional operational loads. The loading diagram can be seen in Figure 8.

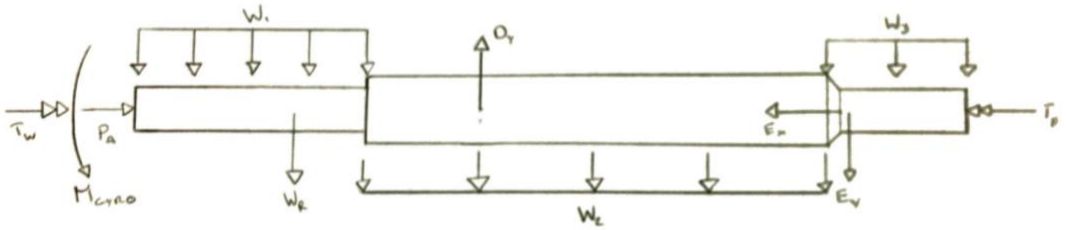

Figure 8. The Loads Used in the Shaft Design.

The values for all these loads are listed in Table 3. The stresses induced by the combined loading of the shaft were used to determine the necessary diameter. The highest stress concentrations of concern were found at the steps in the shaft. The steps were necessary to locate the hub and to take the axial load on the

shaft. The turbine experiences relatively small loading, so a minimum shaft diameter of 8mm was chosen for the purposes of machinability. The shaft design provides a safety factor of 24.8 for the determined loads. The thicker shaft means deflections will be minimized, which also reduces the vibrations in the turbine. The distance between the bearings is maximized to decrease the loads on the bearings. The material chosen for the shaft was 1566 Carbon steel for its strong material properties, cost, machinability, and relatively high endurance limit. For ease of assembly, a wrench flat was included on the shaft.

Table 3. Applied and Reactionary Forces on the Shaft.

Load	Value	Units
Weight force of the front portion of the shaft until the first step	0.012	N
Weight force of the shaft from the first step to the first bearing	0.036	N
Weight force of the shaft between the two bearings	0.063	N
Weight force of the shaft after the second bearing	0.0080	N
Weight of the rotor components	5.56	N
Axial force from the wind	29.80	N
Gyroscopic moment	0.17	N*m
Torque due to the wind	0.40	N*m
Vertical reaction at the first bearing	12.10	N
Vertical reaction at the second bearing	6.37	N
Axial reaction at the second bearing	29.80	N
Torque applied by the generator	0.40	N*m

2.4.2 Shaft Analysis

The critical operational limits on the shaft are the allowable deflections at the bearings, rotor, and coupling. Based on the loading conditions described in Table 3 above, the deflections, stresses, and fatigue on the shaft were found iteratively using an Excel code. The calculated deflections were less than 0.001 degrees for both bearing locations, which are well within the limits specified by the bearing manufacturers. Additionally, the team aimed to minimize deflection of the shaft at the tip as this will lead to whirl. The deflection at the tip of the shaft was also determined to be less than 0.001 degrees, which is sufficiently low to be considered negligible. Lastly, the deflection at the coupling to the generator shaft was also found to be less than 0.001 degrees, well within the tolerance of the coupling. The deflection and yield strength were tested using static load testing, where no deflections or yielding were observed.

2.4.3 Bearings

The shaft required two bearings to accommodate both the axial and radial loading on the shaft. The front bearing needed to hold a 12-millimeter shaft and take a radial load of 15.3 Newtons, while the rear bearing had to hold an 8-millimeter shaft, take an axial load of 29.8 Newtons and a radial load of 9.6 Newtons. Because the loading on the turbine is small, acceptable bearing types narrowed to high-speed ball bearings. This can be an issue at higher loads but is negligible for this design. After selecting NTN radial deep groove ball bearings that fulfilled the loading and sizing requirements, CPWP analyzed the fatigue life. The team found the loading would provide a life far larger than the required design life.

2.4.4 Rotor Balancing Mechanism

The objective of the rotor balancing system is to minimize mass imbalance in the wind turbine's rotor assembly and optimize power collection while meeting safety requirements. The team assumed the sliding

masses were in the plane of the rotor to significantly simplify the analysis. This was accomplished using a grooved plate mounted on the main shaft of the turbine and secured to the hub, which is shown in Figure 9.

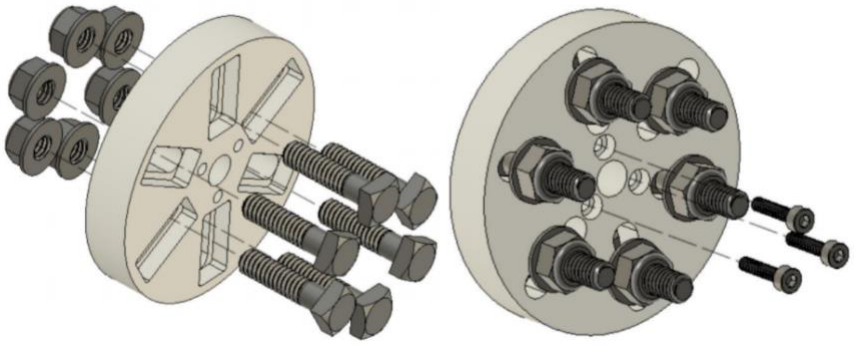

Figure 9. Grooved Plate Rotor Balancing Mechanism Exploded View.

The grooves in the plate allow CPWP to adjust sliding masses in a controlled way, using increments as small as can be measured and accurately maneuvered. The imbalance is measured using an accelerometer mounted to the bearing block, and that information is then fed into a MATLAB program to determine which masses to move and where to move them.

2.5 Support Structures and Yaw

The support structures on the turbine include the tower, base connection to the wind tunnel, nacelle baseplate, and nacelle covers. The yaw mechanism was integrated with the support structure and nacelle.

2.5.1 Tower Design and Analysis

The tower of the turbine consists of a tower column, a tower base dimensioned to the competition requirements, and three ribs to connect the column to the base. The ribs are thin sheet metal cut into triangles, welded to the base and tower to support the tower column. The tower column consists of a steel circular tube to house wires and connect to the yawing mechanism. The tower system was principally concerned with deflection, vibrations, and buckling; finite element analysis was performed, as seen in Figure 10, and it was verified that the system would be functional and meet required deflection limits.

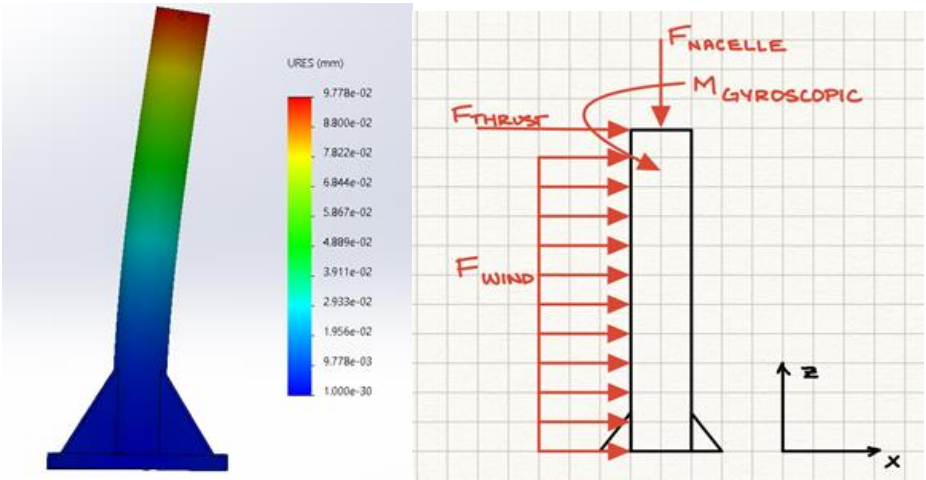

Figure 10. FEA for the Tower, Ribs, and Baseplate. Includes a Radial Thrust Force, Axial Force from the Nacelle, and Pressure Force from the Wind.

2.5.2 Yawing Mechanism and Vane Design

A passive yawing mechanism, which included a rotational mechanism and yaw vane, was utilized to ensure the turbine is oriented into the wind, minimizing yaw error and maximizing power production. For the rotational mechanism shown in Figure 11a, a slew bearing was chosen because it could handle radial, axial, and moment loads with a high factor of safety and minimal friction while also minimizing the number of custom parts needed to be manufactured. The slew bearing connected directly to the nacelle's baseplate, using washers as spacers to eliminate component rubbing, and an internal flange was designed to interface between the slew bearing and tower. The slew bearing was sized based on the static and dynamic loads calculated as well as the tower diameter and wire clearances.

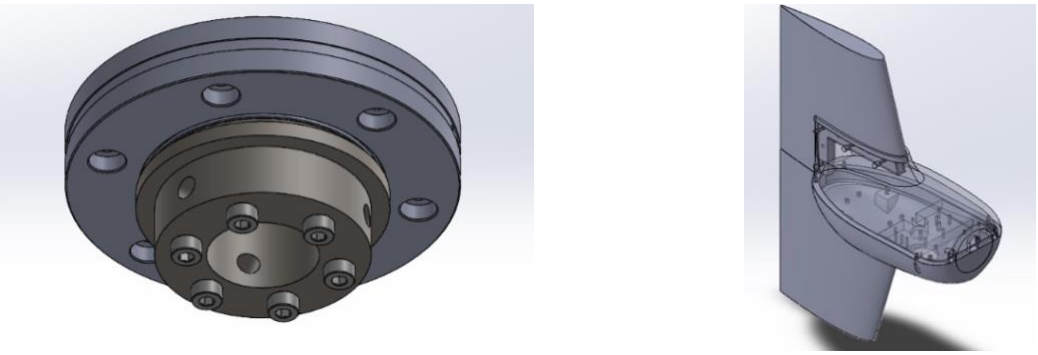

(a) Slew Bearing and Flange Subassembly (b) Yaw Vane and Nacelle Integration

Figure 11. Yaw Mechanism System Components.

Moreover, forces on a yaw vane create a restoring moment that is critical for orienting the turbine. The yaw vane, shown in Figure 11b, was designed to achieve a high drag force when experiencing yaw error by maximizing the surface area with an integrated attachment into the nacelle. Additionally, the yaw vane utilizes a symmetric airfoil cross section, NACA 0015, rather than a flat plate to provide an additional lift force in order to reorient the turbine. The nacelle covers and vanes were produced via a 3D printer and are made of polylactic acid (PLA).

2.6 Electrical Systems Objectives

The turbine's electrical system allows the mechanical rotational power harnessed by the blades to be converted into electrical power. This electrical power is then dissipated across an electrical load. In addition, the electrical system needs to be able to control the speed of the turbine rotor to ensure the system does not exceed its rated rotor speed during high wind speeds. It also must also be able to stop the blades from moving in the event of an emergency. This requires the turbine to continuously sense the power output and rotor speeds to detect if the wind exceeds 11 m/s or a load disconnection has occurred.

2.6.1 Electrical Systems Overview

The electrical system converts rotational mechanical power to electrical power in a controlled and safe manner that completes the turbine testing tasks. On the turbine side of the electrical system, there is a three phase Permanent Magnet Synchronous Generator (PMSG), a rectifier, and an output capacitor. These components will produce a DC voltage with minimal voltage ripple. To best complete the competition tasks, the turbine side of the electrical system is equipped with an Arduino Uno microcontroller. This microcontroller is powered by a buck boost converter that draws from the output of the rectifier. There is a DC voltage, DC current, and a hall effect rotor speed sensor, allowing the microcontroller to monitor these values. The microcontroller can actuate the pitching motors to set the blades to the desired angle.

The load side of the generator contains a dynamic load. The dynamic load is a resistive load whose resistance can be varied by changing the duty cycle of a pulse width modulation signal input. The load side

of the system has an Arduino Uno microcontroller with its own set of DC current and DC voltage sensors. It is powered by a standard 9V cell battery. This microcontroller can change the resistance of the dynamic load by varying the duty cycle of the input.

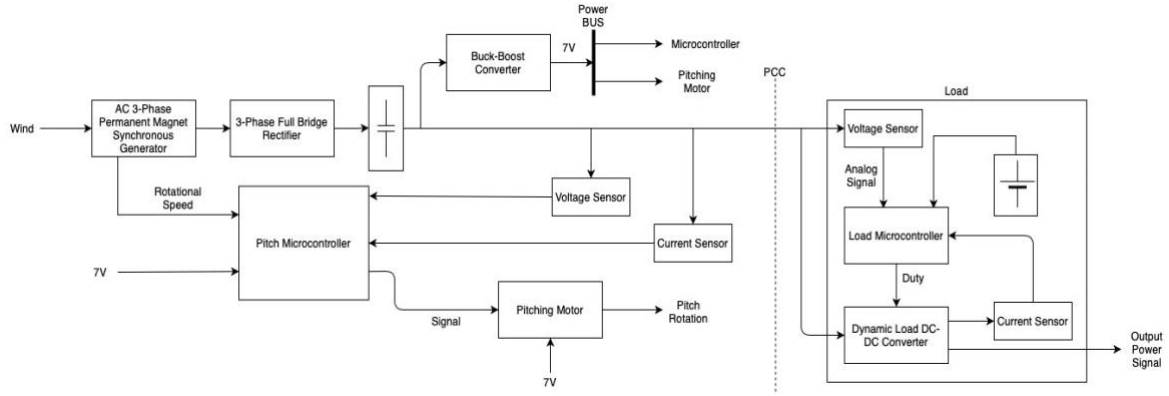

Figure 12. Turbine Electrical System Canonical Model

The electrical system canonical model is shown in Figure 12 and the one-line diagram of the electrical system is shown in Figure 13. The diagram includes the open circuit voltage of the generator (E_G), and the winding resistance. The two diodes represent the pair of diodes that are on at any given point to rectify the three-phase output. The capacitor is used to smooth the voltage ripple. On the load side, a simple potentiometer is used to represent the dynamic load. Both the turbine side and load side of the PCC have a shunt resistor used to sense current.

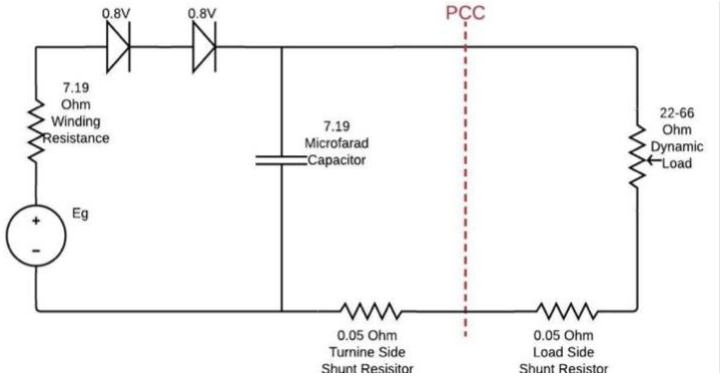

Figure 13. Turbine Electrical System One Line Diagram.

2.6.2 Generator Design and Testing

The generator is the system which converts mechanical rotational power into electrical three-phase AC power. Ideally, the team would have designed and manufactured a generator in house to meet the desired specifications, however, it was decided to purchase this component off the shelf due to uncertainty in the team's ability to secure the lab space needed to manufacture a generator, and as a freshman team in the competition, CPWP wanted to spend more time on other parts of the turbine design. Learning from all-team calls and past competition reports, the team was able to assemble a set of criteria that the generator should meet. The primary concerns noted at the all-team call for off-the-shelf generators were the inability for some generators to produce enough voltage and generators with high cut-in wind speeds. To make sure the generator is producing enough voltage to power a microcontroller, the team wanted to choose one with a low K_V rating. To ensure that the generator could cut in at a low wind speed, a generator with a slotless stator was needed. A slotless stator eliminates the iron teeth that coils are typically wound around, virtually eliminating the cogging torque that could prevent the rotor from spinning at low wind speeds.

In addition to these criteria, the team wanted the generator to have a hall effect sensor. This sensor gives the microcontroller measurements on how fast the rotor is spinning. This information is critical for the control of rated rotor speed task and determining the estimated wind speed. To regulate PCC voltage to at or below 48V, the simplest and most efficient option was to have a generator that would never produce a voltage that high. Since the design of the turbine was to pitch the blades to regulate the rotor speed at wind speeds greater than 11 m/s, the maximum rotor speed the generator should spin at is the optimal TSR rotor speed at 11 m/s. The rotor speed at optimum TSR during an 11 m/s wind speed was expected to be 2100 RPM. To add room for error, the generator should not reach 48 V until the rotor is spinning at more than 3200 RPM. If the K_V rating of the generator is $K_V > \frac{3200\,RPM}{48V}$, thus $K_V > 67\frac{RPM}{V}$, the voltage at the PCC should never reach 48V. The generator selected that met all of these criteria is manufactured by Maxon Motors. The key specifications are listed in Table 4.

Table 4. Maxon EC-Max 40 120W Generator Part# 283873

Specification	Value
K_V [rpm/V]	76.1
Terminal Resistance Phase to Phase [Ω]	7.19
Rated Power [W]	120
Rated Voltage [V]	48

The team used an at home dynamometer test setup built in house, pictured in Figure 14, to spin the shaft of the generator. Although the generator was purchased off-the-shelf, this test setup was useful to verify that the generator was operating in agreement with the specifications laid out in the data sheet. In addition, this setup enabled the team to test the hall effect sensor integrated into the generator body.

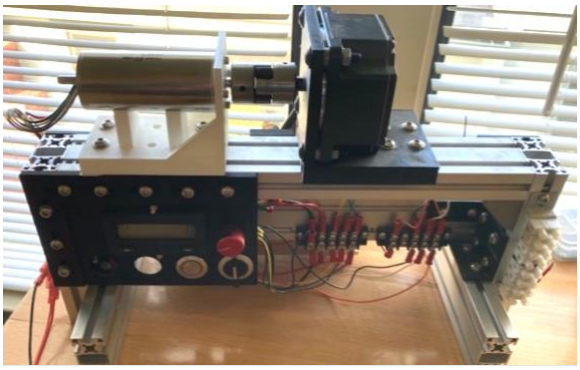

Figure 14. Cal Poly's Custom Dynamometer Test Setup. Generator (left) Coupled to Dynamometer (right).

The results of the dynamometer testing are shown in Figure 15. The generator power output and rectified DC voltage were measured at various rotor speeds and resistive loads. The dynamometer was only capable of spinning up to a speed of 2800 RPM, so to verify that the PCC voltage would never exceed 48V, a trendline was extrapolated to 3200 RPM as shown in Figure 15b.

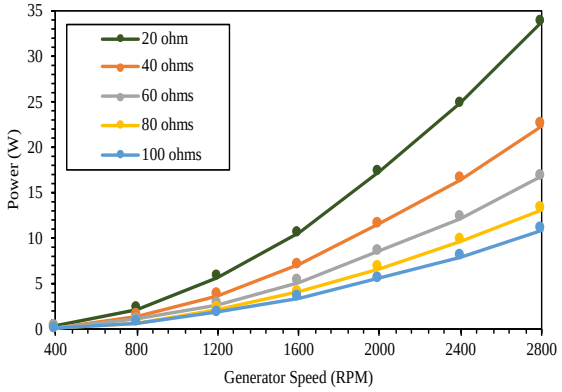

(a) Load Power vs. Generator Speed

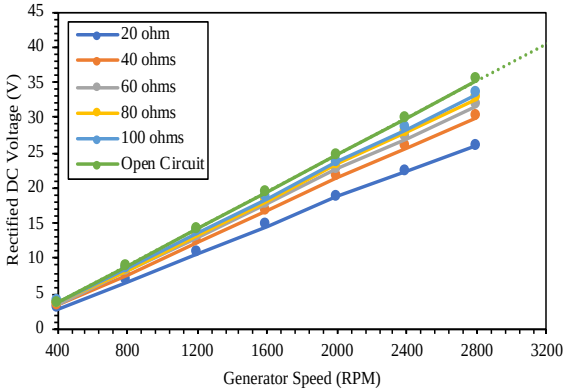

(b) DC Voltage vs. Generator Speed

Figure 15. Dynamometer Testing Results

2.6.3 Hall Effect and Current Sensors

A hall effect sensor provides generator rotor speed information from magnetics inputs. The team utilized the hall effect sensor that was included with the generator to acquire information about the turbine's rotor speed in RPM. These RPM measurements are essential in the control of rated rotor speed task. A basic voltage divider was built to allow the Arduino Uno microcontroller to measure the voltage at the output of the rectifier without damaging it. Additionally, a current sensor was included to measure power by multiplying the sensed voltage and current, and to sense load disconnection. If voltage is detected at the output of the rectifier, but no current is sensed, the microcontroller knows the load was disconnected and shuts down the system.

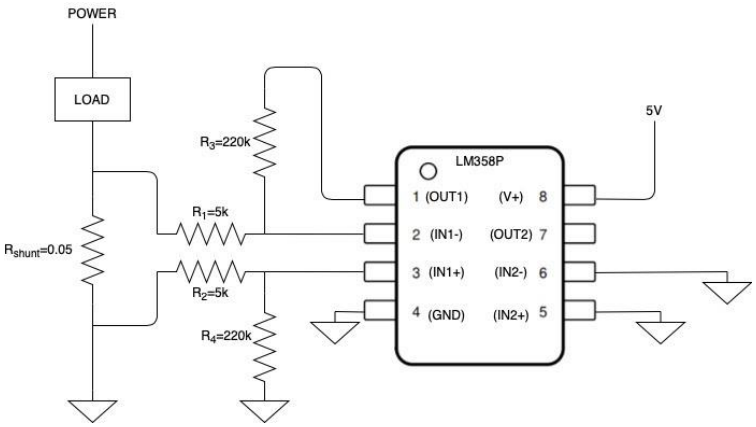

Figure 16. Circuit Schematic of Shunt Resistor Based Current Sensor.

The current sensor was designed and built-in house. The circuit schematic is shown in Figure 16. The design utilizes a low-side shunt resistor and a differential amplifier. This design allows the turbine and load side microcontrollers to sense up to 1.75 Amps of DC current flowing through the PCC.

Figure 17 shows the testing results of the shunt DC current sensor. The testing results demonstrate that the sensor saturates at a current of approximately 1.75A, which is greater than the highest expected current. Additionally, the plot shows the power loss as a function of current. It is important that the current sensor undergoes minimal losses to maximize the turbine's performance in the power performance curve task. The power loss reaches a value of about 150 mW at 1.75A.

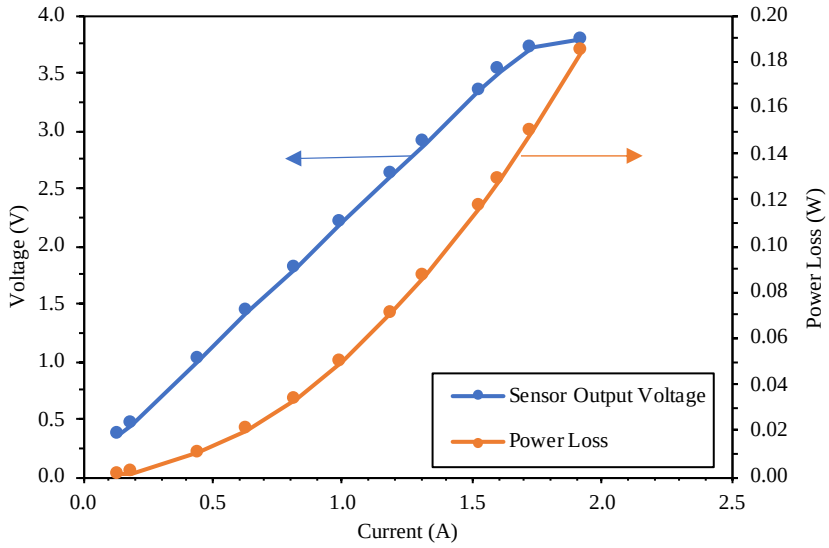

Figure 17. Power Loss and Output Voltage vs. Current Testing Results of Current Sensor

2.6.4 Load Design and Analysis

As the wind speed changes, the resistance that will produce the greatest output power changes as well. In order to maximize the output power, a dynamic load, as shown in Figure 18a, whose resistance can be varied was designed. A resistance range of $66\Omega - 22\Omega$ was chosen by reviewing loads successful teams have chosen in the past, and by analyzing the wind tunnel test data.

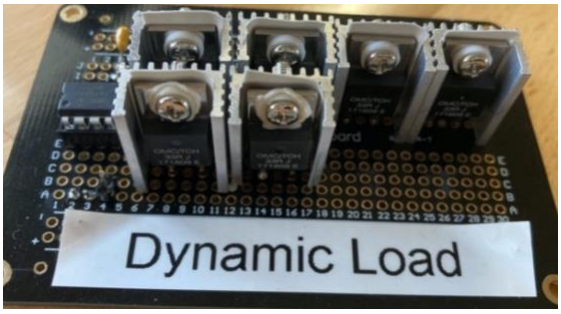

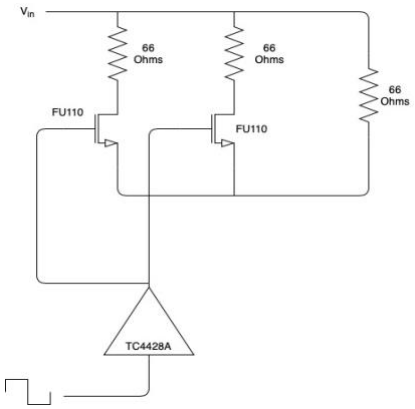

(a) Manufactured Component (b) Circuit Schematic

Figure 18. Dynamic Load Component and Circuit Schematic

A circuit schematic of the dynamic load can be seen in Figure 18b. The system changes the average resistance by quickly switching on and off two resistors in parallel with the third. When the NMOS devices are on, the equivalent resistance is 22Ω. When the NMOS devices are off, the equivalent resistance is 66Ω. As the duty cycle increases from 0% to 100%, the resistance drops from 66Ω to 22Ω. This relationship can be seen in the testing data plotted in Figure 19. The FU110 power NMOS was chosen because it could operate in saturation mode with a gate voltage of 5V, the output voltage of the Arduino that will be driving them. In addition, a gate driver was needed to switch the gates on and off quickly.

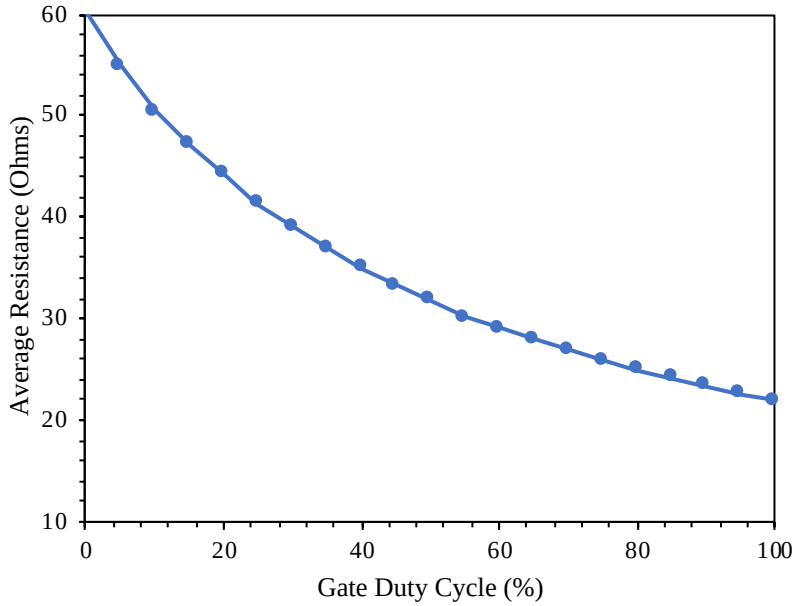

Figure 19. Dynamic Load Average Resistance vs. Gate Duty Cycle Testing Results

2.6.5 Buck Boost and Voltage Regulation

To supply sufficient power and regulate voltage to the control electronics, a buck-boost controller was selected. Specifically, the LM5145RHFEVM-HD 4-Switch Buck-Boost Controller Evaluation Module from Texas Instruments was chosen. This controller was selected for turbine-side voltage regulation because it has a wide-range input voltage range: $5.5V\ -\ 42V$. This allows for power to be drawn from the main power (generation) line post-rectification to supply voltage to the turbine side Arduino and pitching actuators. This module offers adjustable feedback control to deliver constant voltage at its output. The control system and pitching actuators require $7V$ to be delivered from the Buck-Boost controller. This output is adjusted by changing feedback resistor values. According to the user manual, the appropriate feedback resistor for the desired output voltage can be achieved using the following equation.

$$R_{FB1} = \frac{R_{FB2}V_{ref}}{V_{out} - V_{ref}} = \frac{(100{,}050\ [\Omega])(0.8\ [V])}{7\ [V]\ -\ 0.8\ [V]} = 12.910\ [k\Omega]$$

A feedback resistance of $13k\Omega$ was selected to yield an output voltage of $7V$. This resistor was soldered onto the Buck-Boost Controller Evaluation Module to tune the output voltage.

2.6.6 Controls Analysis and Software Documentation

In order to complete the turbine testing tasks to the best of the team's ability, the electrical system is equipped with a turbine and a load side microcontroller. The function of these microcontrollers is to mimic the power output vs wind speed curve shown in Figure 20 by altering blade pitch and load resistance.

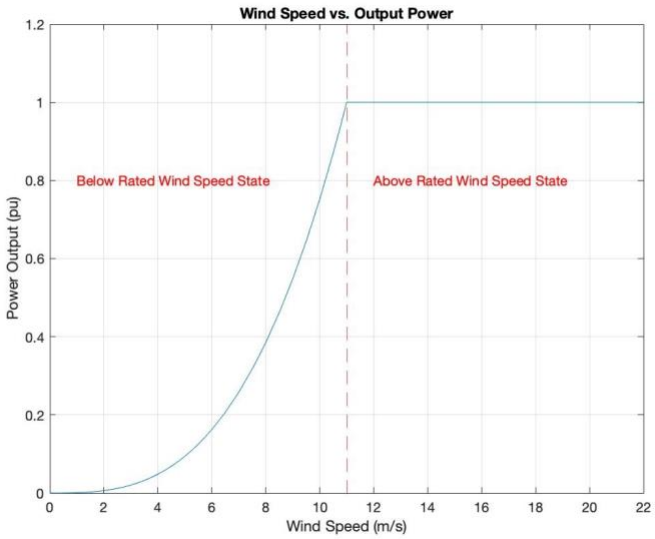

Figure 20. Plot of Ideal Wind Speed vs. Power Output

The turbine side microcontroller is programmed as a finite state machine with three states: below rated wind speed state, above rated wind speed state, and the shutdown state. A microcontroller finite state machine diagram is shown in Figure 21. The microcontroller switches between the below and above rated wind speed states when the power crosses above or below the rated power threshold. This threshold is the experimentally determined power output of the wind turbine at 11 m/s. At any time during the below or above rated wind speed states, the E-stop button may be pressed, or the load may be disconnected. If this happens, the load microcontroller transitions to the shutdown state where the blades are pitched out of the wind indefinitely, slowing the rotor to a standstill. In the below rated wind speed state, the blade pitch is held at a constant angle of attack.

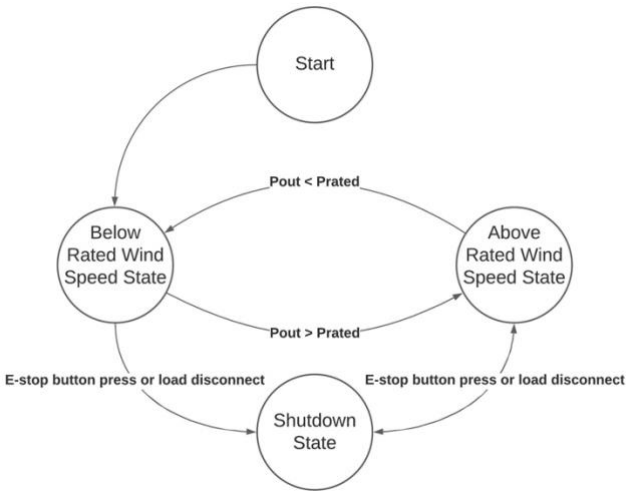

Figure 21. Load Side Microcontroller Finite State Machine Diagram

In the above rated wind speed state, a Proportional and Integrative (PI) control loop scheme, as shown in Figure 22, is used to regulate both rotor speed and output power at the same values measured during an 11 m/s wind speed. In this PI loop utilizes the blade pitch mechanism as an actuator and the hall effect rotor speed sensor as the feedback path. The PI system is able to correct disturbances, such as the wind speed increasing from 12 m/s to 13 m/s, to settle the rotor speed to the "rated" 11m/s value. By regulating the rotor speed of the generator, the voltage output will remain constant, and therefore the power due to the resistive load will also remain constant.

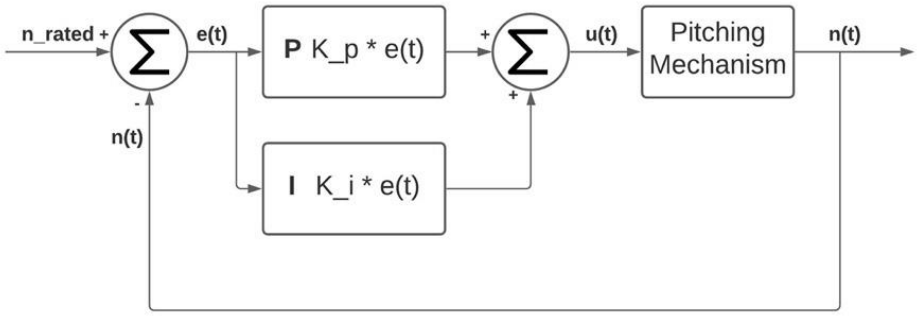

Figure 22. Turbine Side Microcontroller Above Rated Wind Speed State Control System

The load side microcontroller uses its current and voltage sensors to calculate the power being supplied to the load. The microcontroller can change the resistance of the load to increase the power output. It utilizes a lookup table that will be populated with optimum resistances at each integer wind speed. These optimum resistances are found by varying the resistance of the load at various wind speeds and pitching the value which yields the greatest power.

3.0 TESTING

Testing of the turbine and its subsystems was one of the major challenges the team faced because of the health restrictions and severely limited access to campus facilities and labs. Despite this, the team utilized some creative methods to validate the designs and assess the overall turbine performance.

3.1 Field Testing

Most of the testing performed on the turbine can be considered as field testing, since it was done in less controlled environments like students' backyards and out of car sunroofs. Subsystem and component tests are discussed in their relative report sections and in the Testing Milestone Report. At the beginning of the competition, the team did not have access to a wind tunnel, so a small setup was built in a student's garage with a large cardboard box propped in front of a fan. Using a handheld anemometer, the team was able to measure the wind speed exiting the box and placed the chosen rotor set on a basic unloaded turbine setup at varied distances from the end of the box to measure the approximate cut-in wind speed. Originally, the team was interested in maximizing the startup torque of the turbine, and as such chose to continue to refine the best performing blade since it had lower cut-in wind speed in this initial test.

The next set of testing was done with the electrical system connected to the turbine and a dynamic variable load. This test was performed by placing the turbine nacelle components out of the top of a car sunroof. The voltage and amperage produced at various resistances was measured using a multimeter, and the car was driven slowly up to about 14 m/s, verifying that the prototype was capable of withstanding the wind speeds it would later experience in the Cal Poly aerospace department's wind tunnel. This also verified that the blade and rotor design was capable of producing power properly.

With the new capacitors in place, the team was able to test the turbine with a new more powerful fan up to about 10 m/s. This test was inherently variable since the team did not have access to the tunnel to streamline the airflow, but it was powerful enough to show that the rpm of the blades needed to nearly double to reach the power output desired for the given generator. Since the blades were 3D printed, the team decided to go back to the drawing board and re-design the blade airfoils and TSR. The team found a new set of airfoils to evaluate in QBlade. The resulting theoretical best performing airfoil was placed in the in-house blade design code and new geometries were defined. Six different blade geometry variations were printed and tested again in front of the powerful fan to determine the best rotor geometry for the turbine.

The ability of the turbine to have a stable yaw in variable wind speeds was evaluated on the Cal Poly campus during a particularly gusty day. The passive yaw system was able to realign the turbine quickly when manually rotated out of the incoming wind direction, quickly aligning itself to the incoming wind direction within the 180º per second rule requirement.

3.2 Wind Tunnel Testing

Following the car sunroof testing, the fixed-pitch prototype turbine was tested for the first time within the actual wind tunnel. This was again effective at showing that the fixed-pitch rotor could produce power, albeit lower than desired by the team. The data collected was used to optimize the resistance of the load at various wind speeds and showed a significant amount of oscillation in recorded power. This was identified as a ripple effect from the rectified three phase AC voltage and was addressed by adding the capacitors to the system (they were still being shipped at the time of first testing). The data is plotted in Figure 23a.

The final wind tunnel test at the time of this report again utilized a fixed hub turbine, but with the final blade geometry determined using the large fan testing mentioned above. A laser tachometer was also used to verify that there was no slippage between the drivetrain and the generator, and to gather data to associate the wind speed with the rotor rpm. The power curves produced are shown in Figure 23b.

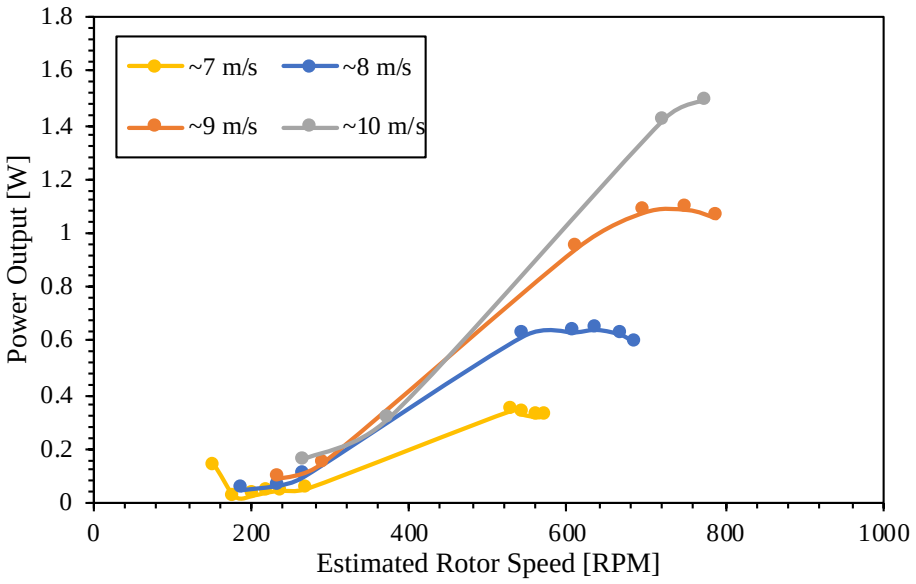

(a) Wind Tunnel Test #1 with SG6043 Airfoil

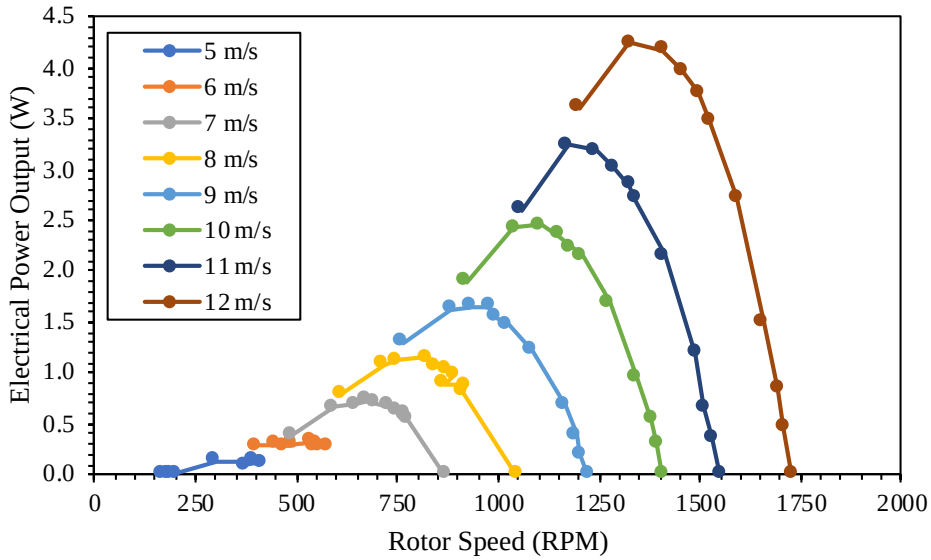

(b) Wind Tunnel Test #2 with New SD7043 Airfoil

Figure 23. Wind Tunnel Testing Turbine Performance Results – Output Power vs. Rotor Speed

An important thing to note about the second wind tunnel test is that the blades were about 1.5 cm undersize in length. This was due to the accessible 3D printer beds not having a large enough build volume to print the full length blades. This also indicates that the turbine should be able to generate more lift and thus higher rotational speeds. With the full-size blades, the turbine is assumed to generate more power.

At the time of this report the team was not able to complete full wind tunnel testing with the pitching mechanism installed due to unexpected shipping issues for necessary bearings; however, the pitching mechanism and the turbine with a static hub were tested extensively and perform as anticipated.

4.0 CONCLUSION

Through testing, the team has learned what caused the turbine to produce less power than anticipated: namely the selection of a rated speed for a generator that was higher than the blades can achieve. The tradeoff of establishing a low cut-in wind speed in place of higher power at the rated was emphasized too heavily. The team now knows how to change the generator selection and blade tip speed ratio in future iteration of the design. Despite these issues, CPWP was able to make marked improvements in the performance of the turbine over the course of the current testing up to this point. The team plans to fully incorporate the pitching mechanism to improve performance even further before the end of the competition.

The wind turbine designed by Cal Poly Wind Power was successful in meeting most of the design goals outlined by the team and competition. It produced less power than desired, however, the design process undertaken by the first-year team has provided an excellent groundwork which can be taken and improved to reach the power production goals. Analytical tools such as the electrical and controls schematics, and rotor optimization MATLAB script can be modified and utilized by future Cal Poly CWC teams. The turbine paved the way for Cal Poly to use a variable-pitch system in the future which can be optimized with further testing.

5.0 REFERENCES

[1] US Department of Energy. (2020) CWC 2021 Rules and Requirements. Collegiate Wind Competition 2021

[2] Manwell, James F., et al. (2011) *Wind Energy Explained: Theory, Design and Application*. Wiley.

[3] Anderson, Collin G. (2020). *Wind Turbines: Theory and Practice*. Cambridge University Press.